Development of a Conceptual Model for Vadose Zone Transport of Tc-99 at Hanford's BC Cribs and the Screening of Remedial Alternatives- 9458

A. L. Ward and R.J. Serne
Pacific Northwest National Laboratory
Richland, Washington 99352

M.W. Benecke
CH2M Hill Plateau Remediation Company
P.O. Box 1600, Richland, WA 99352

ABSTRACT

A number of waste trenches and cribs at Hanford's BC Cribs and Trenches site, which received about 10 Mgal of scavenged tank waste with elevated concentrations of technetium-99 and nitrate, are being evaluated for remediation. The objectives of this study were to: 1) develop a conceptual model for vadose zone transport of mobile contaminants, and 2) investigate the effects of fine-scale heterogeneity (i.e. horizontal laminations, cross-bedding) on the large-scale transport behavior with the goal of developing an appropriate remedial strategy. The vertical heterogeneity structure, conditioned on grain size distributions and borehole geophysical logs (water content and natural isotopes), was developed from a single borehole at the site. Geostatistical methods were used to impose a 3-D spatial correlation structure, using information from an adjacent well-characterized experimental site, and to merge heterogeneities at various scales. Flow and transport properties were derived using property transfer models based on grain size distributions. The STOMP simulator was used to predict flow and transport through the vadose zone and into a 5-m thick confined aquifer during the period of trench operations (1956-1958) through to the present time. Results show that fine-scale heterogeneity within the large-scale lithologic units enhanced lateral flow and mixing, limited vertical penetration in the vadose zone, and played a critical role in keeping contaminants above the water table. Model results show good agreement with a contaminant profile from a borehole installed in the 216-B-26 trench. Simulated distributions of nitrate and electrical resistivity are also in good agreement with the results of a field-scale resistivity survey. These results suggest that installation of an engineered surface barrier would reduce the threat to ground water by reducing the mass flux of contaminants to the water table and increasing the residence time in the vadose zone.

INTRODUCTION

The BC cribs and trenches form a group of liquid waste disposal sites located south of Hanford's the 200 East Area in the 200-TW-1 operable unit (OU). Waste sites within this OU received scavenged waste from the uranium recovery and ferrocyanide processes at the 221/224-U Plant, which recovered the uranium from the metal-waste streams at the B and T Plants, and liquid wastes from 300 Area laboratory operations (1). Waste discharges to this site were on the order of 30 Mgal with possibly the largest inventory of ^{99}Tc ever disposed to the soil at Hanford. To date, there is no verifiable evidence of contaminants in the groundwater, and owing to uncertainties in the waste inventory, the fate of contaminants released at the site was also uncertain. There was, however, evidence of surface contamination attributed to animal intrusion in one of the 200-TW-1 OU waste sites. The 216-B-26 Trench was recently characterized to augment existing information related to geology and contaminant distribution and to support an accelerated cleanup schedule. Data from the 216-B-26 characterization provided significant insight into the vertical distribution of contamination in the vadose zone. Much of the contamination is now known to still be in the vadose zone, thereby posing a possible long-term source for groundwater contamination. Remediation is being

accelerated at these wastes sites but development of an effective remediation plan and the evaluation of remedial options will require a detailed analysis of fate and transport for this site.

Historically, liquid-waste disposals to the ground at the U.S. Department of Energy's (DOE's) Hanford Site have relied on models to predict the fate and transport of chemicals discharged in the liquid effluents. Early models used for discharge calculations were relatively simple and were based on the concept of specific retention (2). It was typically assumed that the waste discharges would move readily into the vadose zone and be retained by the sediments and that recharge was negligible in the site's semi arid climate. It was recognized that lateral spreading of contaminants could take place, but this phenomenon was typically ignored in the calculations of specific retention (1,2). Present day observations of contaminant plumes are significantly different from predictions with simple models. Recent groundwater-monitoring data suggest that contaminants associated with liquid discharges and tank leaks are in the groundwater beneath some waste sites at Hanford (3). Yet, at other sites that received similar volumes of effluent discharges of similar chemical composition and exposed to identical meteorological conditions (e.g. rainfall and snowmelt), contaminants are in the vadose zone, high above the water table. Recent sampling at the 216-B-26 Trench shows a zone of ^{99}Tc contamination between 18 and 53 m. The peak soil concentration exceeds 100 pCi/g while the pore water concentration is approximately $1.4 \cdot 10^6$ pCi/L, with both peaks occurring around 30 m (1,4). The current distribution of ^{99}Tc in the vadose zone beneath 216-B-26 is therefore not easy to explain using current conceptual models. The retention of large concentrations of ^{99}Tc high above the water table is indicative of strong stratigraphic controls on the downward migration. With an accurate conceptual model, it should be possible to identify the volumes or areas of soil to which remedial actions would be necessary.

Current conceptual models ignore small-scale lithostratigraphy and treat the porous media as homogenous and isotropic. Simulations with these models suggest that migration of waste from specific retention trenches would be rapid and mostly vertical with mobile contaminants reaching the unconfined aquifer within weeks of discharge (1). Current hypotheses for the discrepancy between model predictions and field observations include an overestimation of scavenged waste discharges to the trenches and/or extensive lateral spreading of the contaminant plume in the near surface. Rejection of either hypothesis is essential to developing the most appropriate conceptual model and a remediation strategy for the site. For the BC Trench site, such confirmation is possible with a detailed analysis of the features, processes, and events at the 216-B-26 Trench.

P
SCOPE AND OBJECTIVES

The scope of the study was to develop containment alternatives for remedial actions and evaluate these alternatives against a no-action alternative and eliminate those that would be unable to meet remediation goals. Evaluation of the alternatives requires a good understanding of the active fate-and-transport mechanisms to support development of the most appropriate conceptual model. Thus, the objectives of this study were to: 1) develop a conceptual model for vadose zone transport of mobile contaminants, and 2) investigate the effects of fine-scale heterogeneity (i.e. horizontal laminations, cross-bedding) on the large-scale transport behavior with the goal of developing an appropriate remedial strategy. The resulting conceptual model would then be used with a numerical model to evaluate the potential magnitude of leachate releases from the vadose zone and the potential for future horizontal and vertical migration of these contaminants.

CP
CONCEPTUAL MODEL

The conceptual model describes the important features, events, and processes controlling fluid flow and contaminant transport at the waste site of interest. Development of the conceptual model is perhaps the most critical step in modeling contaminant fate and transport. In developing the conceptual model, all available information on the site features, events, and processes relevant to the BC Trench site was reviewed.

Hydrostratigraphy

The site is located in 200 East Area of Hanford's central plateau. The hydrogeology of the 200 Area has been extensively studied. The vadose zone beneath the 200 East Area can be subdivided into five principal hydrostratigraphic units, including three Hanford-formation units and two units belonging to the Ringold Formation (5). The Hanford formation units include 1) an upper-gravel-dominated Hanford formation, 2) a sand-dominated Hanford formation, and 3) a lower-gravel-dominated Hanford formation (5). Other features include clastic dikes which have been observed in the Hanford formation beneath 200 East Area (6,7). A common assumption in modeling flow and transport in these sediments is one of homogeneity and isotropy. Owing to the depositional environment, these sediments show a distinct microscale structure characterized by the presence of multiple sedimentary layers which manifest as a complex layered and anisotropic system at the macroscopic scale. The Hanford formation typically contains relatively thin fine-textured lenses that could enhance lateral spreading of water and contaminants and reduce the vertical movement of contaminants (Fig. 1). Fine-textured lenses typically have low vertical permeabilities and higher horizontal permeabilities. Low-permeability layers within the Hanford formation are relatively thin (0.5 m or less) and laterally discontinuous with frequent pinch outs (**Error! Reference source not found.**).

At wastes sites with this type of heterogeneity, the geometry and configuration of sedimentary, hydrologic, and geochemical facies are difficult to define without extensive excavation and sampling. These heterogeneities, however, can be captured by coupling high-resolution borehole logs with less-frequent grain-size distributions through property transfer models. Neutron moisture logs, for example, have proven useful stratigraphic indicators (8). Theory predicts that coarse-textured soils generate relatively low neutron counts while fine-textured silt and clay layers generate much higher counts. Neutron moisture measurements, which were made in the undisturbed medium at a resolution of about 3 inches, clearly show the effects of small-scale stratigraphy.

Figure 1. Exposed Trench Face Showing Layered Heterogeneity in Hanford's 200 East Area near to the BC Cribs and Trenches Site.

Thus, neutron logging can be a cost-effective reconnaissance tool to locate specific, potential, or suspected flow paths in existing wells or borings that are not continuously cored or sampled. The neutron moisture and natural gamma logs from C4191 and surrounding boreholes were therefore central to the development of the hydrostratigraphic model for the site. Accurate simulation of flow and transport must therefore account for the

small-scale lithostratigraphy with adequate description of the local-scale hydraulic properties and saturation-dependent anisotropy mechanisms. Failure to account for these heterogeneities, which manifest as thin layers, would likely result in an underestimation of lateral spreading and an over-estimation of the penetration depth.

Flow and Transport Properties

In such heterogeneous formations, detailed characterization of the flow and transport properties and their variability are the minimum requirements for predicting field-scale flow (9). Required properties for variably saturated flow include the soil moisture characteristic, i.e., the water content-capillary pressure relationship, □(□); and the unsaturated hydraulic conductivity versus capillary pressure relationships, K(□), including parameters for describing saturation-dependent anisotropy. No hydraulic properties were measured on the samples from the C4191 borehole and no undisturbed samples were available for characterization but a number of representative samples were selected for grain-size analysis based on observed contrasts in water content. With no site-specific hydraulic properties, the grain-size statistics obtained from the analysis of selected grab samples were used to estimate properties using property transfer models (PTMs). These PTMs assume that the relationships between moisture content, pressure head, and unsaturated hydraulic conductivity are non-hysteretic and can be represented by the Brooks-Corey (10) water-retention and relative-conductivity model.

Accurate predictions of flow and transport also require detailed characterization of the transport parameters, particularly dispersivity, □. Dispersivity is well known to be scale-dependent and to depend on soil texture. Recent studies have show that the longitudinal dispersivity, $\square_L$, increases as $\square_b$ increases and as □ decreases (11). These values, however, are local-scale values and are expected to be smaller than the values needed to predict field-scale behavior. Local-scale estimates of $\square_L$ were assigned to individual layers based grain size statistics and on *in situ* moisture content. The transverse dispersivity, $\square_T$, was assumed to be 0.1 $\square_L$.

PTMs for the different textures were derived using a combination of data from site measurements (12,13) and other published data (14,15) from which relationships between size statistics and hydraulic properties could be derived. The resulting PTMs were used to estimate the saturated hydraulic conductivity, K_s; saturated water content, $\square_s$; the Brooks-Corey pore size distribution index, □; air entry pressure, $\square_b$, $\square_T$, and $\square_L$ (1). Calculated parameters are summarized in Table I. The adsorption of Tc(VII) is low under nearly all conditions relevant to the Hanford vadose zone and upper unconfined aquifer; a K_d of 0 mL/g was assigned to both technecium-99 and nitrate.

Table I. Estimated Brooks-Corey Parameters for the Various Strata at the BC Trench Site

USDA Texture Class	Mean Diameter (mm)	$\square_s$	$\square_r$	$\square_r$	$\square_a$ (cm)	□	K_s cm/hr	$\square_L$(m)	$\square_T$(m)
Sand	0.6713	0.437	0.020	0.046	15.98	0.69	21.0	0.0073	0.00073
Loamy Sand	0.4357	0.437	0.035	0.080	20.58	0.55	6.11	0.0154	0.00154
Sandy Loam	0.2068	0.453	0.041	0.091	30.2	0.38	2.59	0.0291	0.00291
Loam	0.0576	0.463	0.027	0.058	40.12	0.25	1.32	0.0516	0.00516
Silt Loam	0.0293	0.501	0.015	0.030	50.87	0.23	0.68	0.0753	0.00753
Sandy Clay Loam	0.0915	0.398	0.068	0.171	59.41	0.32	0.43	0.0291	0.00291
Clay Loam	0.0292	0.464	0.075	0.162	56.43	0.24	0.23	0.0516	0.00516
Silty Clay Loam	0.0129	0.471	0.04	0.085	70.33	0.18	0.15	0.0681	0.00681

A representative flow-and-transport model of the BC trenches was therefore developed to be multidimensional and included: 1) representation of the small-scale stratigraphy and the site-specific ranges in physical and chemical properties (based on available geologic, soil physics, and geochemical data from nearby boreholes and outcrops);

tilted layers to accommodate the natural slope to the formation; and 3) representation of lateral spreading along multiple strata with contrasting physical properties (e.g., bedding contacts), which appears to be prevalent within the fine-grained lenses. The water table is located at 103.17 m below the surface and a 5-m thick confined aquifer was assumed beneath the water table. For the aquifer, the hydraulic conductivity was set to 1,615 m/day whereas the effective porosity was set to 0.26. A hydraulic gradient of 0.001486 m^{-1} was assumed with a mean groundwater velocity of 0.24 m/day and a dispersivity of 1 m.

Contaminant Release and Recharge History

Six trenches in the immediate vicinity of the 216-B-26 Trench were operational during the same time frame as 216-B-26. These include 216-B28 and 216-B-27 to the south and 216-B-25 through 216-B-23 and 216-B-52 to the north. Median fluid discharge volumes and contaminant inventories, derived from the SIMS model (16) are summarized in Table II. Discharges were generally short, lasting from 30 days to 90 days. The mean volume was just over 4000 m^3, except for the much larger 216-B-52 Trench, which received over 8500 m^3 of fluid. Trenches 216-B-23 through 216-B-28 received median values of ^{99}Tc ranging from 16 to 18 Ci while 216-B-52 received over 25 Ci.

Table II. 2004 Composite Analysis 10,000-year (Median Inputs)
Assessment of Fluid Discharge Volumes

Trench	Length (m)	Start Date	End Date	Duration (days)	Vol (m^3)
216-B-52	176.78	12/01/57	01/01/58	31	8529.52
216-B-23	152.40	10/01/56	10/31/56	30	4519.90
216-B-24	152.40	10/01/56	11/01/56	31	4869.87
216-B-25	152.40	11/01/56	12/01/56	30	4909.90
216-B-26	152.40	12/01/56	02/01/57	62	4745.64
216-B-27	152.40	02/01/57	04/01/57	59	4419.88
216-B-28	152.40	04/01/57	06/30/57	90	5049.79

Table III. 2004 Composite Analysis 10,000-year (Median Inputs) Assessment for ^{99}Tc (Ci)

Year	Technecium-99 Influx by Trench						
	B-52	B-23	B-24	B-25	B-26	B-27	B-28
1955	0.0000	0.0000	0.0000	0.0000	0.0000	0.0000	0.0000
1956	0.0167	0.0000	0.0476	0.0000	14.2491	0.0452	0.0476
1957	6.1197	15.3636	18.1086	18.0399	3.3504	16.4384	17.3002
1958	19.3691	0.0000	0.0000	0.0000	0.0000	0.0000	0.0000
1959	0.0000	0.0000	0.0000	0.0000	0.0000	0.0000	0.0000
Total	25.5044	15.3636	18.1086	18.3099	17.5995	16.4836	17.3678

Recharge rate is controlled by climate, topography, soil type, and vegetation and is generally small in vegetated shrub-steppe ecosystems (17). However, it can be quite important, particularly when the potential for long-term contaminant remobilization is considered. In extremely wet years, or on bare surfaces, significant amounts of water may move out of the root zone, creating the potential for deep drainage and contaminant transport. Historical aerial photos show that the site was covered predominantly with grasses and sage brush before installation of the trenches.

A recharge rate of 3.5 mm yr^{-1} was selected as the initial recharge rate, which is consistent with that of a mature shrub-steppe community (17). Trench construction would have removed vegetation resulting in an increase in

Table IV. 2004 Composite Analysis 10,000-Year (Median Inputs) Assessment for NO_3^- (kg)

Year	Nitrate Influx by Trench						
	B-52	B-23	B-24	B-25	B-26	B-27	B-28
1955	0.0	0.0	0.0	0.0	0.0	0.0	0.0
1956	0.0	802052.7	959358.7	966725.6	751029.6	0.0	0.0
1957	321183.5	0.0	0.0	0.0	177256.6	871113.6	916344.3
1958	962740.7	0.0	0.0	0.0	0.0	0.0	0.0
1959	0.0	0.0	0.0	0.0	0.0	0.0	0.0
Total	1283924.2	802052.7	959358.7	966725.6	928286.2	871113.6	916344.3

recharge. For that period, a recharge rate of 50 mm yr^{-1} was assigned. The trenches were backfilled on decommissioning and, over time, vegetation invaded the surfaces. Recharge decreased to a range consistent with a mixed surface of shrubs and grasses; a value of 25 mm yr^{-1} was assigned based on measurements from the prototype Hanford barrier. These data show an average recharge rate of 18 percent of precipitation on a sparsely-vegetated gravel cover (18).

NUMERICAL SIMULATIONS

Simulations focused on predicting the distribution of ^{99}Tc and NO_3^- through the vadose zone to the water table. The initial condition was established by simulating steady flow from time zero to the year 1956 with a constant recharge rate of 3.5 mm yr^{-1}. Recharge rates were allowed to vary as a function of precipitation during trench operations of the trenches and after decommissioning. The steady flow solution was then used as the initial condition for the transient flow and transport analyses. To best represent conditions at the site, the transient simulations were simulated in two stages. In the first stage, flow and solute transport were simulated with opened trenches that were subject to natural precipitation. In this stage, nodes representing the trenches were made inactive, and the required boundary condition was applied over the trench bottom. The second stage represented the period after trench operations following backfilling of the trenches. During this stage, the inactive trench nodes were converted to active nodes with a material type identical to that surrounding the trenches. Simulations were performed with the PNNL-developed STOMP90 simulator (19) with the Portable Extensible Toolkit for Scientific Computation (PETSc) solver.

Solution Domain

The physical domain consisted of a 2-D north-south cross section through trenches 216-B-52 at the north to 216-B-28 to the south. This section, which is equivalent to section Q`-Q`` (20) that provided the gross stratigraphy for the site. Small-scale heterogeneities were derived from grain-size distributions, in conjunction with high-resolution neutron logs from surrounding boreholes, using geostatistical methods. The sequential Gaussian simulation routine **SGSIM** from **GSLIB** (21) was used to generate realizations of volumetric water content on a 70 by 1317 node mesh of the computational domain. The parameters of the variogram models developed for the 299-E24-111 Experimental Test Well located in the eastern section of the 200 Area Plateau of the Hanford Site were used as input in the sequential Gaussian simulation. The variogram model for the 299-E24-111 site shows that the maximum direction of continuity was in the northeast direction (22.5 degree) with a range on the order of 100 m. The southeast direction (112.5) showed a trend and a much shorter range of about 15-20 m. The field-measured water contents were assumed equivalent to the specific retention, which is controlled by texture. These data were used to estimate grain-size statistics, which then used to estimate flow and transport properties using PTMs. The physical domain was discretized using a Cartesian grid with variable horizontal and vertical spacing. The domain was

bounded on the south by Well 299-E13-12 and on the east by Well 299-E13-51. The domain consists of 78 nodes in the x-direction; 71 in the y-direction, and 1322 in the vertical, giving a total of 7,321,236 nodes. The computational domain extended over a distance of 200 m in the west-to-east direction, and 250 m in the north-south direction. Thus, the vertical extent of the computational domain was set at 108.17 m. The vertical spacing in the current model is 0.075 m, but can be increased by upscaling the properties.

Boundary Conditions and Source Terms

In all of the simulations, a no-flow boundary was imposed at the bottom of the domain, representing the base of the 5-m thick confined aquifer at 108.17 m. Vertical boundaries on the north, east, south, and west were specified as zero-flux boundaries for water flow and solute transport. For the 2-D north-south transect, groundwater was assumed to flow in a southerly direction under a gradient of $1.486 \cdot 10^{-3}$ m/m. Thus, the south boundary of the aquifer was treated as a hydraulic gradient boundary that allowed water and solutes to flow out. The north boundary of the aquifer was treated as a Neumann boundary with a steady influx of water at a Darcy velocity of 0.24 m/day.

The source terms consisted of fluid and contaminant discharges to the series of trenches during trench operations. Estimated fluid volumes and inventory are defined by the median values predicted by the SIM model (16). Fluid discharges are reported to have started in late 1956 and ended in early 1957 for most trenches, except for the 216-B-52 Trench, which was operational into 1958. A total of 37,044 m^3 (37 million liters) of fluids were applied during the operational period. On average, Trenches B-23 through B-28 received around 4752 m^3, while the much longer B-52 received 8529 m^3. To facilitate the evaluation of the impact fluids and contaminants originating from one trench on another, the fluids were injected into each individual trench. All fluid releases in the simulations originated at the base of the trench, and no ponding was allowed. The injection rate for input into STOMP was calculated by dividing the injection rate by the number of nodes covering the source area. The rate per unit linear length of trench was then divided by the number of nodes (n = 6) extending over the width of the trench bottom to generate the source strength for each node. All contaminants were assumed to be dissolved in the discharged fluids; thus, the time history is identical to that of the fluid releases.

REMEDIAL ALTERNATIVES

CERCLA § 121(b)(1), 42 U.S.C. § 9621(b)(1) mandates that remedial actions must be protective of human health and the environment, cost-effective, and use permanent solutions with alternative treatment technologies and resource recovery alternatives to the maximum extent practicable. These objectives are based on available information and standards, such as applicable or relevant and appropriate requirements (ARARs) and risk-based levels established using the risk assessments. A major remedial-action objective of relevance to the BC trench site is to maintain ^{99}Tc levels in the groundwater at values below the groundwater ARARs. The ARARs for groundwater are 900 pCi/L for ^{99}Tc and 10 mg/L for NO_3^-. There are a number of potentially suitable treatment technologies and process options for radiologically contaminated soils that could be applied to the BC trench site to minimize the long-term downstream transport of ^{99}TC and NO_3^-. These general response actions include: 1) no action, 2) monitored natural attenuation, 3) soil excavation, 4) offsite disposal, 5) soil washing, 6) *in situ* vitrification, 7) onsite containment and capping. To support a feasibility study, such general response actions must be screened for effectiveness, implementability, and relative cost. In evaluating the alternatives, the goal was to determine the extent of chemical impacts on soil and groundwater; identify underlying soil and groundwater flow patterns, and select the most feasible cleanup alternative. Thus, the resulting conceptual model was used to screen the alternatives and identify those that would minimize the long-term downstream transport of ^{99}TC and NO_3^-. This naturally limited the analysis to evaluation of onsite containment and capping.

The no-action alternative provides an environmental baseline against which impacts of any proposed action and the alternatives can be compared. For the BC cribs and trenches, the no-action alternative consists of refraining from the active application of any remediation technology. At present, the trench surfaces are bare to sparsely vegetated with no infiltration controls. The no-action alternative also assumes no source-control removal action, no infiltration

control, no revegetation, no administrative actions (including institutional controls), and no monitoring. One simulation, Case 1, was performed to evaluate the no-action alternative. The onsite capping alternative involves placement of an engineered cap consisting of fine-textured high-storage capacity material on top of the contaminated site after placement of a layer of fill. The fine-textured material minimizes recharge by storing precipitation until it can be recycled to the atmosphere by plants. This alternative would also rely on naturally occurring attenuation processes to reduce the toxicity, mobility, and mass of the contaminants in the subsurface but does not include the removal of contaminated sediments. At the time of this analysis, capping alternatives had not been identified. Consequently, no specific candidate designs are considered. Modeling was conducted to evaluate the impact of infiltration control on the target levels for groundwater over a 10,000-yr period. Table V summarizes the simulation cases.

Table V. Summary of Simulation Cases for Evaluation of Alternatives

Case	Description	Start Date	End Date	Recharge Rate (mm/yr)			
				Pre-op	Operation	Post-Op	Remedial
1	No Action	2012	10012	3.5	77.0	25.0	25.0
2	No Action	2012	10012	3.5	77.0	25.0	3.5
3	Cap A	2012	10012	3.5	77.0	25.0	0.5
4	Cap B	2012	10012	3.5	77.0	25.0	0.1
5	Cap C	2012	10012	3.5	77.0	25.0	0.0

The main difference between the five cases results from differences in the drainage criterion for the barriers. Cap A is the least robust of the covers and is assumed to restrict recharge to 1.0 mm yr^{-1} for the duration of the simulation. Cap B is assumed to limit recharge to 0.5 mm yr^{-1}, the same as the prototype Hanford barrier. Cap C is the most robust of the three with a drainage criterion of 0.0 mm yr^{-1}. For each remedial alternative, model simulations were performed to determine the extent of chemical impacts on soil and groundwater; to identify underlying soil and groundwater flow patterns, and to select the most feasible alternative. Simulations were executed for a periods of compliance ranging from 500 years to 10,000 years. Initial flow conditions for the first stages of the simulation were established with a steady-state flow simulation that assumed a natural infiltration rate of 3.5 mm yr^{-1}.

RESULTS AND DISCUSSION

Simulation results show that the characteristics of the flow field and the distribution of moisture are controlled by lithostratigraphy, hydraulic properties, and the presence of subsurface features, e.g., sloped or pinched layers that can focus or redirect flow. Natural precipitation and its temporal distribution is also important as short-term fluctuations can cause large localized saturation changes. Such effects are not evident in analyses that ignore the fine-scale heterogeneity.

Distribution of Moisture and Contaminants During Trench Operations

Figure 2 shows the predicted distribution of moisture and aqueous ^{99}Tc in 1958 on January 01, 1958, just after the discharges to 216-B-52 had ended. This trench received almost twice the average volume received by the other six trenches. Despite some 37,045 m^3 of water having been added at this time, it is still mostly in the top 20 m of sediments. The region around the trench (northing = 210 m) is essentially saturated but there is no evidence of water moving past the 20 m depth (Fig. 2a). In fact, most of the waste water appears to have been redistributed laterally in the shallow subsurface, to merge with the plumes from the adjacent trenches. A plot of the mass flux of water across the water table show that the mean flux density (recharge rate) across the water table remained at the pre-Hanford value of 3.5 mm yr^{-1} until 1988. After 1988, the simulations showed a sharp increase in the flux density at the water table. However, this was not water discharged to the trenches but the antecedent moisture that was pushed ahead by the trench discharges. The concept of a specific retention dictates that a soil column can only hold a finite amount of water against the force of gravity and any water in excess of this amount will drain. The flux

density continued to increase, reaching a maximum of about 56 mm yr^{-1} in the year 2004. Simulations show a subsequent decrease in flux density at the water table with the value returning to around 3.5 mm yr^{-1} by 2345.

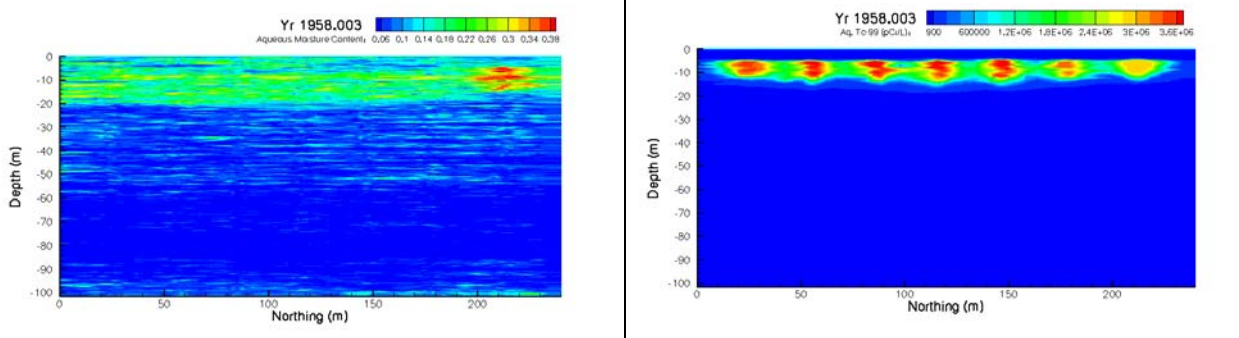

Figure 2. Calculated Distributions of Water Content and ^{99}Tc Along a North-South Transect in at year 1958.003 During Trench Operations

The only evidence of the large 37,045 m^3 discharge of waste water would have been an increase in the concentrations of some ions in the groundwater as the resident pore water entered the water table. However, the simulations show that none of the waste water crossed the water table. The simulated domain was assumed to have a 3 percent dip to the south, which was accommodated in the simulations with a tilted grid. This dip played an important role in the redistribution of water in the subsurface and as such, the mass flux of water across the north and south boundaries were quite different from that observed at the water table. Owing to the dip to the south, flow was predominantly to south, even though the sequence of trench filling appears to have near the north; 216-B-23 and 216-B-24 were the first to become operational. Flow across the south boundary quickly reached a peak rate of about 17.5 L day^{-1} in early July (t = 1957.56), shortly after 216-B-26 ceased operations. Flow across the boundary has since shown a steady decline except for a few spikes in response to changes in surface boundary conditions.

Figure 2b shows the distribution of ^{99}Tc in the pore water in early January 1958 (t=1958.003) shortly after the end of discharges to the 216-B-52 trench. This corresponds to the water distribution shown in Figure 2a. The ^{99}Tc is assumed to be completely dissolved in the pore water and assumed to be conservative with zero K_d. The same assumptions apply to NO_3^- and because the two species are assumed to have identical diffusion coefficients, the spatial distributions were essentially similar. Unlike previous analyses in which small-scale stratigraphic changes are ignored, these simulations show that the mobile species moves laterally with the water and remains high above the water table, even after 50 years in the ground. The pattern of migration of ^{99}Tc and NO_3^- across the boundaries should therefore mimic that of water to a large extent. In fact, break through curves for ^{99}Tc and NO_3^- crossing the south boundary in response to trench discharges showed several sharp changes in concentration that coincide with those observed in the water flux. In general, high fluxes of water resulted in reductions in the ^{99}Tc concentration. This can be expected since ^{99}Tc is transported in the water. These changes are mostly due to changes in surface boundary conditions. However, observed multimodal features are also partly related to the heterogeneity. Lateral flow would be expected to dominate until the potential gradients were sufficient to overcome the entry pressure of underlying coarse layers. Simulations show that the peak in mass flux occurred several years after the discharges ended. The peak ^{99}Tc crossing the south boundary occurred in mid 1985 with a aqueous concentration of $1.79 \cdot 10^6$ pCi L^{-1}. This is about an order of magnitude higher than the peak concentration of $3.2 \cdot 10^5$ pCi L^{-1} observed in 1962 shortly trench discharges ceased. The breakthrough of nitrate showed a similar pattern to behavior to ^{99}Tc; migrations were primarily to the south and none entered the groundwater.

The presence of small-scale textural discontinuities such as those observed in Figure 1 is responsible for the variations in moisture contents observed in the neutron-probe measurements. These heterogeneities may have led to the development of complex flow networks whose impacts dominated those resulting from the large-scale

heterogeneity that is typically the focus of transport simulations. The characteristics of these flow networks appear to vary with input flux and boundary type. The results provide new insight into the interpretation of existing contaminant distribution, field-scale experiments, and the design of remedial systems for contaminated soils. Changes in saturation can completely change the subsurface flow network, thereby influencing the spatial correlation structure of relative permeability and the location of fast paths. This suggests that solute transport may be strongly dependent on saturation in a way more complicated than the simple effect on the pore-water velocity. In such systems, the amount of lateral spreading observed would strongly depend on the flow regime. There is experimental evidence that shows that the horizontal permeability of laminated silts from the Hanford vadose zone can be over 70 times the vertical permeability (7).

These factors have important consequences for field-scale transport and remediation. Contaminants deposited under a massive leak or discharge of waste water, as with the BC cribs and trenches, would show preferential lateral movement initially due to a combination of large lateral potential gradients and large horizontal saturated conductivities. At the much lower natural recharge rates, lateral potential gradients would be significantly smaller. Even though saturation-dependent anisotropy predicts an increased tendency for lateral migration, the hydraulic conductivity at low water contents may be too low to significantly affect redistribution at the low potential gradients. This is of particular importance to the fine-textured lenses that currently show higher water contents in the field. Even though the hydraulic conductivity is higher than that of drier adjacent sands, the actual values of conductivity are such that continued lateral migration would be at very low rates. However, significant vertical migration would also require conditions that were wet enough to overcome the natural capillary breaks.

Present-day Distribution of Contaminants

Figure 3 shows the predicted distribution of ^{99}Tc at the beginning of 2005. In general the predicted plume is located between 20 and 50 m bgs. The current conceptual model suggests that the discharges from the seven trenches initially moved laterally to merge into a single plume. Natural recharge then leached the trailing edge of the plume downward effectively reducing the concentration of the mobile contaminants in the 0 to 20-m depth to background levels. The plume shows some effects of the heterogeneity in that it is asymmetric and multimodal. Under 216-B-26 where the C4191 borehole was installed (northing =110 m) the plume is located between 23 and 50 m bgs. Figure 3 shows an overlay of the electrical resistivity contours derived from a surface resistivity survey conducted at the site in 2003 (22). The distribution of resistivity, a reflection of the distribution of ionic solutes, is in good agreement with the distribution of nitrate. Owing to the similarity in the transport behavior of ^{99}Tc and NO_3^-, the electrical resistivity profile is also correlated with ^{99}Tc. However, it should be noted that in the absence of the high nitrate concentrations, it is unlikely that a resistivity survey would have be able to delineate the plume.

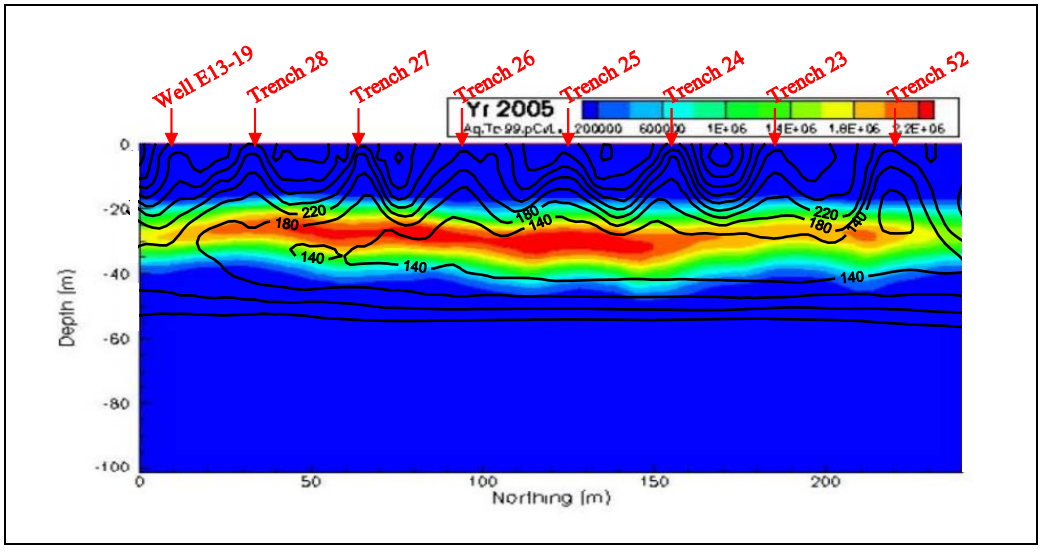

Figure 3. Calculated Distributions of Aqueous ^{99}Tc in the Year 2005 Overlain by Electrical Resistivity Contours from Surface a Resistivity Survey.

In the absence of multidimensional plume distribution data, comparisons between the simulated and observed ^{99}Tc distribution are based on data from the C4191 borehole. In order to make this comparison, we extracted a 1-D profile beneath the 216-B-26 trench at the approximate location of the C4191 borehole. Figure 4 compares the predicted depth profiles for NO_3^- and ^{99}Tc with the measured profiles at the location of borehole C4191. The general trends are remarkably similar given the uncertainty in hydrologic properties and the lack of hydrologic characterization data. The predicted distributions of NO_3^- and ^{99}Tc are remarkably similar to the field observations. In both cases, the predicted center of mass is quite similar.

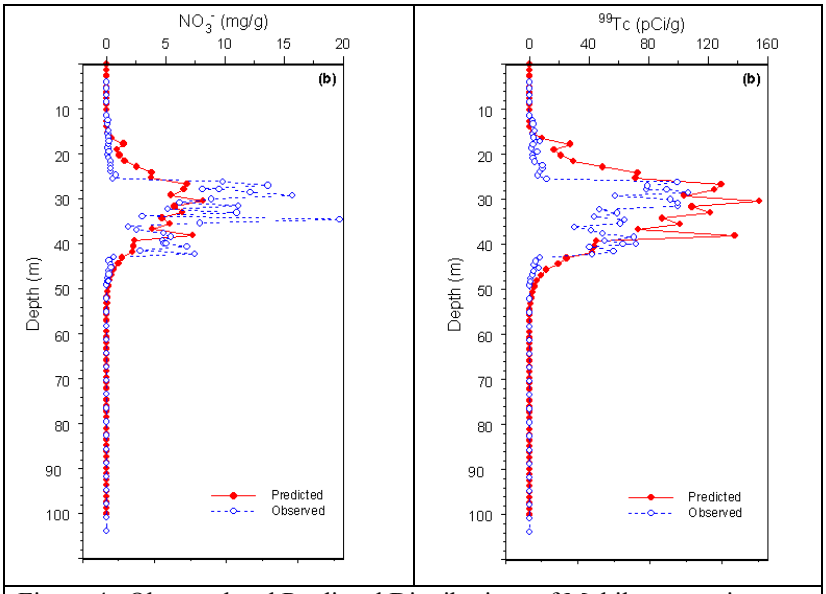

Figure 4. Observed and Predicted Distributions of Mobile contaminants at Borehole C4191 in 2005 (a) aqueous NO_3^-, and (b) and (b) ^{99}Tc.

The center of mass of the predicted ^{99}Tc and NO_3^- plumes is located around 30 m, and the leading edge of the plume extends to around 50 m as in the case of the measured plume. These plots show the effects of small-scale heterogeneities on the contaminant profiles, which is a reflection of depth variations in water content and bulk density. While the model captures the leading edge of the plumes quite well, the trailing edge appears to have been insufficiently leached, thereby giving an apparently larger value of dispersion. First, the model appears to underestimate the concentration NO_3^- whereas it slightly overestimates the concentration of ^{99}Tc. For nitrate, the predicted peak concentrations based on the input inventory is about 1/3 that of the observed. Given that the transport behavior of ^{99}Tc and NO_3^- are expected to be similar, the amount of dispersion in an advection dominated environment would be expected to be similar.

These discrepancies could be due to a number of factors. First, the local longitudinal (vertical) dispersion of contaminants is strongly dependent on the measurement volume. Consequently, dispersion appears smaller when derived from small sampling volumes, such as boreholes, than for the volume of field samples at which large-scale results are desired. Thus, the apparent dispersion derived from measurements in the C4191 borehole can be expected to be smaller than those predicted by the model. Another factor that could contribute to this discrepancy is the dimensionality effect. In the field, horizontal redistribution leading to solute mass accumulation where local flow converges and depletion where it diverges is entirely possible. However, using a 2-D profile for the simulations limits the extent to which redistribution can occur. Only transient multidimensional simulations are capable of producing the actual concentration values that are observed in the field that drive local processes,

including chemical reactions and diffusion. While both of these factors may be responsible for the differences in predicted concentrations, the simultaneous prediction of higher apparent dispersion with a higher peak concentration creates a dilemma. The fact that predicted total ^{99}Tc is higher than the observed, even though dispersion is greater, suggests that the inventory used as input may be too high. Similarly, the only possible explanation for the lower predicted NO_3^-, in the absence of decreased dispersion, is an underestimation of the input NO_3^- inventory. Similarly, the over estimation of the ^{99}Tc is also likely due to an inventory estimates, in this case and over estimations. The source concentrations of ^{99}Tc and NO_3^- were both derived from the median values from the SIMS (16) model runs. Given that the solution to the transport equation is linear, it could be solved for a unit mass of input and scaled to the appropriate input value until the actual concentrations match. An adequate match between the observed and predicted could be achieved by reducing the input inventory by around 50 percent. An alternative approach would be to optimize the source strength by inverting the observed concentration profile. Nevertheless, the fact that the difference in peak concentration is only 50 percent, even with uncertainty in inventory and model dimensionality, is again quite remarkable. The C4191 borehole, however, cannot provide any validation of the extent of spreading predicted by the model. Confirmation can come only from further sampling or from non-invasive geophysical logging that can delineate the extent of the plume. It is expected that as such data become available revisions would be made to the conceptual model to minimize any discrepancies between observations and model simulations.

Performance of the Capping Alternative

Figures 5a and 5b compare the predicted mass flux of ^{99}Tc and NO_3^- at a receptor 100 m down-gradient of the source for the no-action and capping alternatives. With the current conceptualization and model parameters, the first arrival of ^{99}Tc occurs at the receptor in 2118 at the 25 mm/yr recharge rate. A peak concentration of $2.09 \cdot 10^4$ pCi/L arrives in 2228. A recharge rate of 25 mm yr^{-1} leads to a peak ^{99}Tc concentration of $3.6 \cdot 10^5$ pCi L^{-1} reaching the water table in the year 2095. Nitrate shows similar trends although the first arrival is generally earlier due to the larger concentrations of NO_3^- and the relatively low MCL. At the 25 mm/yr, the MCL for NO_3^- reaches the water table in 2125. In all cases, the concentration reaching the water table increased with a decreasing recharge. The increase in concentration can be expected because a reduction in pore water velocity would cause a reduction in the dispersion coefficient. A smaller amount of dispersion would mean higher peak concentrations. Recharge rates used in the simulations were also assumed to be time invariant. This may explain the relatively symmetric nature of the breakthrough curves compared to that observed on the south boundary that was subject to the short-term effects of changes in water flux. It is expected that the use of recharge that is a percentage of precipitation, such that episodic high-flux events can be captured, may produce somewhat different distributions. Such a scenario could see moisture conditions in the soil reaching a level at which the water-entry pressure of coarse layers could be overcome and deep drainage rates increase to bring about episodic entries of ^{99}Tc and NO_3^- into the groundwater.

Figures 5c and 5d show the mass flux of ^{99}Tc and NO_3^- for a 0.1 mm yr^{-1} barrier. In the current conceptualization, the hypothetical barriers were assumed to extend to the boundary of the simulation domain so as to avoid issues related to the design and performance of side slopes on above grade covers. For ^{99}Tc, simulation results showed the arrival of the MCL at the receptor occurs in year 2740 for the 0.1 mm yr^{-1} barrier and not much later in year 2761 for the 0.0 mm yr^{-1} barrier. The relatively early arrivals even with barriers is due to the combined effects of plume depth and the recharge rate assumed to exist until the assumed barrier deployment in 2012. A significant amount of water in the profile would have to redistribute before the full benefits of the barrier were realized. Another unknown but very important factor is the extent of lateral spreading. The current model assumes a spatial continuity of 100 m., which could easily be an under-estimation of the actual degree of spreading. A more accurate assessment would require additional characterization data. The NO_3^- plume shows similar behavior. The first arrival occurred in 2266.29 for the 0.1 mm yr^{-1} barrier and 2266.86 for the 0.0 mm yr^{-1} barrier. Peak concentrations occurred significantly later. Neither the 0.1 mm yr^{-1} barrier nor the 0.0 mm yr^{-1} barrier resulted in peak concentrations reaching the water table even after the year 12005. However, the peak in water flux from the antecedent moisture was discernable bringing the peak concentrations significantly less than the MCLs to the receptor.

Owing to the large inventory of ^{99}Tc and NO_3^-; the high mobility of the two contaminants; and the long half life of ^{99}Tc, the no action case would not remove the threat to groundwater and would be less desirable than capping. Based on the foregoing analyses, capping would significantly delay the arrival of mobile contaminants at the water table but leachate concentrations reaching the water table would be in excess of the MCLs. However, application of

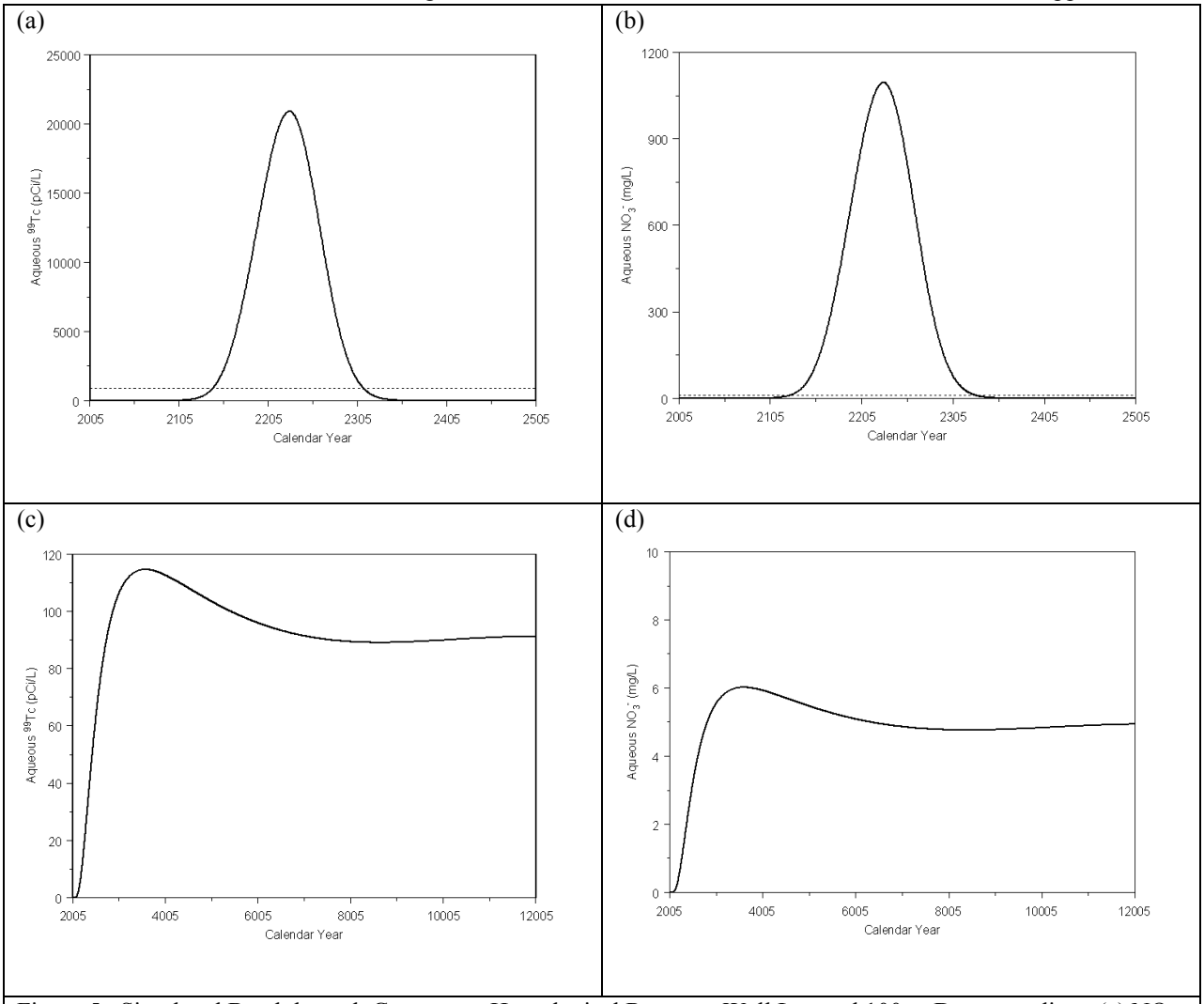

Figure 5. Simulated Breakthrough Curves at a Hypothetical Receptor Well Located 100 m Down-gradient, (a) NO_3^- under the 25 mm yr^{-1} recharge rate no-action alternative, (b) ^{99}Tc under the 25 mm yr^{-1} recharge rate no-action alternative, (c) NO_3^- under the 0.1 mm yr^{-1} recharge rate engineered barrier, and (d) ^{99}Tc under the 0.1 mm yr^{-1} recharge rate engineered barrier.

the soil screening level (SSL) analysis and calculation of dilution attenuation factors for the different recharge rates show that all of the capping alternatives would reduce concentrations of NO_3^- and ^{99}Tc at a receptor well to levels significantly below their MCLs. Both modeling approaches show consistency in the results.

SUMMARY AND CONCLUSIONS

Several intentional waste discharges occurred within the 200-TU operable unit beginning in 1956 and continuing into 1958. By combining the waste-release history for each trench, a gross chronological conceptual model of composite contaminant release to the vadose zone was be generated. High-resolution borehole logs suggest a highly stratified medium with numerous thin fine-textured layers in the top 12 to 15 m and formed the basis of the

stratigraphic model. Property transfer models, based on grain size statistics were used to assigned flow and transport properties at the scale of the borehole logs. Properties are regionalized to a full 3-D simulation domain by variogram modeling, retaining information on small-scale lithologic structure.

Unlike previous analyses in which small-scale stratigraphic changes have been ignored, the mobile species (^{99}Tc and NO_3^-) moved laterally with the water and remained high above the water table, even after 50 years in the ground. STOMP simulations show significant movement of water and contaminants to the south the 216-B-28. Antecedent moisture from the soil column was pushed ahead by the waste water discharges but contained no contaminants. Results show a strong dependence of the structure of subsurface flow networks on recharge rate and saturation with lateral flow dominating under certain conditions. Results also suggest that some regions of the porous medium that were accessible during the initial high-flux discharges may have become relatively inaccessible as desaturation occurred. These regions could again become accessible to infiltrating water only if saturations and fluxes similar to those at the time of trench operations reoccur. This appears unlikely under current and expected recharge scenarios. This combination of factors may explain why ^{99}Tc, more than 50 years after being discharged to the shallow subsurface, is still over 50 m above the water table. Model predictions of the current plume distribution were remarkably similar to field observations. The predicted peak concentration under 216-B-26 was less than 20 percent higher than the peak observed in C4191 samples. The discharges from the multiple trenches appear to have commingled to form a single plume in zone between 20 and 50 m bgs. Having successfully predicted the current location of the plume, there is increased confidence in using the conceptual model to predict behavior under the two remedial alternatives.

Hypothetical engineered barriers significantly delayed first arrival, arrival of the MCL, and arrival of the peak when compared to a no-action alternative. Although leachate concentrations were in excess of the MCls, concentrations at a hypothetical receptor located 100 m down gradient of the site show that drinking water standards would be protected. First arrival and arrival of the MCLs were identifiable for all the caps. However, in spite of running the model out to year 12005, peak concentrations for the 0.1 and 0.0 mm yr^{-1} barriers were indeterminable. These results therefore suggest that on-site capping could be an effective technology, increasing the residence time of mobile contaminants in the vadose zone. Undoubtedly, the range of caps analyzed delayed the arrival times of ^{99}Tc and NO_3^- at the water table significantly beyond those predicted for the no-action alternatives.

Based on the foregoing analyses and the comparison of projected concentrations of mobile contaminants reaching the water table no-action alternatives would fail to reduce contaminant concentrations to soil screening levels. Consequently, concentrations reaching a receptor 100 m down gradient of the waste site would exceed the MCLs and the no-action alternative would fail to eliminate the threat to groundwater.
Owing to the large inventory of ^{99}Tc and NO_3^-, the high mobility of the two contaminants, and the long half life of ^{99}Tc, additional measures will be required to meet the appropriate screening levels or to further increase residence time. An engineered barrier would minimize the threat by increasing the residence time and a reducing the mass flux. Only then would concentrations reaching the receptor would fall below the MCLs.

REFERENCES

1. A.L. WARD, G.W. GEE, Z.F. Zhang, and J.M. Keller. *Vadose Zone Contaminant Fate-and-Transport Analysis for the 216-B-26 Trench*, PNNL-14907, Pacific Northwest National Laboratory, Richland, WA.
2. W.A. HANEY and J.F. HONSTED. *A History and Discussion of Specific Retention Disposal of Radioactive Liquid Wastes in the 200-Areas.* HW-54599, Hanford Atomic Products Operation, Richland, WA (1958).
3. M.J. HARTMAN, L.F. MORASCH, and W.E. WEBBER. *Hanford Site Groundwater Monitoring for Fiscal Year 2003*. PNNL-14548, Pacific Northwest National Laboratory, Richland, WA (2004).
4. R.J. SERNE and F.M. MANN. *Preliminary Data From 216-B-26 Borehole in BC Cribs Area*. RPP-20303, Rev. 0. CH2MHill Group, Richland, Washington (2004).

5. M.P. CONNELLY, B.H. FORD, and J.V. BORGHESE. *Hydrogeologic Model for the 200 West Groundwater Aggregate Area*. WHC-SD-EN-TI-014, Rev 0, Westinghouse Hanford Company, Richland, WA (1992).
6. C.J. MURRAY, A.L. WARD, and J. WILSON. "Influence of Clastic Dikes on Vertical Migration of Contaminants at the Hanford Site". *Vadose Zone J.* 6: 959–970 (2007)
7. A.L. WARD and Z.F. Zhang. "Effective Hydraulic Properties Determined from Transient Unsaturated Flow in Anisotropic Soils". *Vadose Zone J*. 6:913–924 (2007).
8. J.H. KRAMER, S.J. CULLEN, and L.G. EVERETT. "Vadose zone monitoring with the neutron probe." In: *Handbook of Vadose Zone Characterization and Monitoring*. LG Wilson, LG Everett, and SJ Cullen, Editors, Geraghty & Miller Environmental Science and Engineering Series (1995).
9. A.L. WARD, G.W. Gee, Z.F. Zhang, and J.M. Keller. *Vadose Zone Transport Field Study: FY 2002 Status Report.* PNNL 14180, Pacific Northwest National Laboratory, Richland, WA (2002).
10. R.H. BROOKS and A.T. COREY. "Hydraulic properties of porous media." *Hydrol. Pap. 3*, Colorado State University, Fort Collins, CO (1964).
11. E. PERFECT, M.C. SUKOP and G.R. HASZLER. "Prediction of dispersivity for undisturbed soil columns from water retention parameters." *Soil Sic. Soc. Am. J.* 66(3):696-701 (2002)
12. R. KHALLEL and E.J. FREEMAN. *Variability and scaling of hydraulic properties for 200 Area soil,Hanford Site.WHC-EP-0883* Westinghouse Hanford Company, Richland, Washington (1995).
13. S.P. REIDEL and D.G. HORTON. Geologic Data Package for 2001 Immobilized Low-Activity Waste Performance Assessment. PNNL-12257, Rev. 1., Pacific Northwest National Laboratory, Richland, Washington (1999).
14. W.J. RAWLS, D.L. BRAKENSIEK and K.E. SAXTON. "Estimating soil water retention from soil physical properties and characteristics." *Adv. Soil Sci.* 16:213-234 (1982).
15. R.F. CARSEL and R.S. PARRISH. "Developing joint probability distributions for soil water retention characteristics", *Water Resour. Res*. 24:775-769 (1988).
16. B.C. SIMPSON, R.A. CORBIN, and S.F. AGNEW. *Hanford Soil Inventory Model*. BHI-01496 Rev 0 (also LA-UR-00-4050), Bechtel Hanford Inc., Richland, WA (2001).
17. M.J. FAYER. J.E. SZECSODY. *Recharge Data Package for the 2005 Integrated Disposal Facility Performance Assessment*. PNNL-14744, Pacific Northwest Laboratory, Richland, WA (2004).
18. A.L.WARD, S.O. Link, C.E. STRICKLAND, K.E. DRAPER, and R.E. CLAYTON. "200-BP-1 Prototype Hanford Barrier Annual Monitoring Report for Fiscal Years 2005 Through 2007." PNNL-17176. Pacific Northwest National Laboratory. Richland, Washington (2007).
19. M.D. WHITE and M. OOSTROM. STOMP Subsurface Transport Over Multiple Phases, Version 2.0, User's Guide. PNNL-12034, Pacific Northwest National Laboratory, Richland (2000).
20. K.R. FECHT, G.V. LAST, and M.C. MARRATT. Granulometric Data 216-B and C Crib Facilities Monitoring Well Sediments. RHO-LD-45, Rockwell Hanford Operations, Richland, WA (1978).
21. C.V. DEUTSCH and A.G. JOURNEL. *GSLIB: Geostatistical Software Library and User's Guide.* 2nd ed., Oxford University Press, NY (1998).

22. D.F. RUCKER and M.D. SWEENEY. *Plume Delineation in the BC Cribs and Trenches Area.* PNNL-14498. Pacific Northwest National Laboratory, Richland, WA.